

STATIC AND DYNAMIC PROPERTIES OF SHORT, NARROW, VARIABLE-THICKNESS MICROBRIDGES

M. D. Feuer* and D. E. Prober

Becton Center, Dept. Engineering and Applied Science, Yale University, New Haven, CT 06520

ABSTRACT

The electrical properties, including the Josephson-effect response to microwave radiation, have been studied for extremely small, high-resistance microbridges of Pb-In alloy and unalloyed In, with dimensions ranging from 300Å to 2000Å. The $I_c R$ product of In and Pb-In microbridges decreases smoothly as the bridge cross section is reduced, approaching the Ginzburg-Landau limit of 0.64 mV/K for the smallest bridges. The voltage range of microwave response and the temperature range of hysteresis-free operation both increase (improve) as the bridge is made narrower, in agreement with Joule heating theory. For example, an 8 ohm $Pb_{0.9}In_{0.1}$ bridge with all dimensions ≤ 500 Å has a maximum step voltage of $V_{max} = 1.5$ mV and a non-hysteretic temperature range of $\Delta T_{no\ hyst} = 1.2$ K. Bridges of unalloyed In can show still better response due to a longer coherence length, and non-hysteretic operation over the full temperature range below T_c is possible.

I. INTRODUCTION

Superconducting microbridges are an important class of Josephson weak-link devices¹, with significant potential for application in high-frequency detectors and SQUIDS, due in part to their thin-film reliability and potential reproducibility. It has been recognized in recent years that improved microbridge performance, and remedies for some of the significant problems such as Joule heating, could be achieved by making microbridges as small as, and shaped like, high-quality point contacts.^{1,2} In this work, we report on the properties of ultrasmall Pb-In and In variable-thickness microbridges (VTBs), for which all dimensions can be less than 500Å.³ We have studied in detail the limits on the Josephson effect in these devices, and their dependence on material parameters and dimensions. The effect of boundary scattering in very narrow (<400Å) In bridges was also investigated. Other microbridge properties which relate to non-equilibrium effects are discussed in detail elsewhere.⁴

II. FABRICATION AND MEASUREMENT PROCEDURE

The microbridges studied were fabricated in the variable-thickness configuration, to reduce the effects of self-heating, and to localize the depression of the order parameter. The basic fabrication process utilizes the novel two-dimensional shadowing technique based on substrate-step edges of Ref. 3, with subsequent improvements.⁴ A picture of a small In microbridge fabricated with the improved technique is shown in Fig. 1. The width at the center is <400 Å. Other dimensions are in Table II, below.

Films of $Pb_{0.9}In_{0.1}$ and In were used in these studies, as these are well-characterized, soft superconductors. The films were evaporated onto liquid-nitrogen-cooled substrates to achieve small grain size, which for the Pb-In alloy was substantially smaller than that of the In film in Fig. 1 (see Ref. 3, Fig. 1). Material parameters of our films are listed in Table I. One (unintentional) alloy microbridge of $In_{.95}Pb_{.05}$ was produced, but most properties were like those of the Pb alloy bridges, so it is not discussed in detail here.

Manuscript Received Sept. 30, 1980.

*Present address: Bell Laboratories, Murray Hill, N.J.

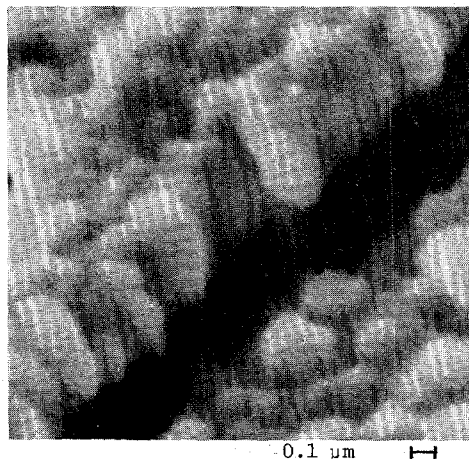


Fig. 1 Scanning electron micrograph of bridge S-14. Minimum width is <400Å. Viewed at an angle.

Attempts to fabricate Sn bridges were not successful due to stress in the film, which led to splitting of the film at the substrate steps.

Measurements of dc $V(I)$ curves were made in an rf and magnetically-shielded cryostat, with carefully shielded, battery-powered electronics and a Keithley nanovoltmeter, as described elsewhere.^{4,5} With the precautions employed, no microbridges were burned out during mounting or routine measurement.

III. MICROBRIDGE PARAMETERS AND CRITICAL CURRENTS

The dimensions and basic parameters of the bridges studied are listed in Table II. The parameter R_d is the minimum differential resistance at $t \equiv T/T_c = 0.99$ (see below). Comparing the characteristic lengths in Table I to the bridge dimensions, it is seen that all of the microbridges tested in this study were sufficiently narrow to be in the uniform-depairing regime⁶ ($L, W < \xi(T)$) over a fairly wide temperature range near T_c . The Pb-In bridges are in the small-bridge dirty-material limit^{6,7} ($\lambda \ll (L, W) < \xi(T)$) for a range of at least 0.5 K below T_c . The pure In films used for bridges S-13, S-14, and S-15, have a mean free path $\lambda = 1450$ Å, determined from the measured resistance ratio, $\rho_{295}/\rho_4 = 13.2$, and the $\rho\lambda$ product.⁸ We thus find that $\xi(0) = 1660$ Å for our In films, with ξ the Ginzburg-Landau coherence length. For both the Pb-In and In films, the T_c and ρ values are in good agreement with bulk values.

As expected, the effect of boundary scattering is easily discerned in the In bridges. The most dramatic case is bridge S-14. From the measured resistance ratio of the (bridge+banks), and assuming the bridge resistance = R_d and that there is a uniform mean free path ℓ_b in the bridge region, we find that $\ell_b = 70$ Å and $\xi_b(0) = 370$ Å for bridge S-14. Values of $\xi_b(0) = 730$ Å and 1520Å apply for bridges S-13 and S-15, respectively. As seen in Fig. 1, the In bridges in fact do not have a uniform cross section, and we expect that scattering occurs primarily in the narrowest region. Still, values of ℓ_b calculated above are a useful guide.

Critical currents, $I_c(T)$, of all the microbridges are observed to be a linear function of temperature over a fairly wide range near T_c , as expected theoretically.^{6,7} $I_c(T)$ for a narrow Pb-In bridge is shown in

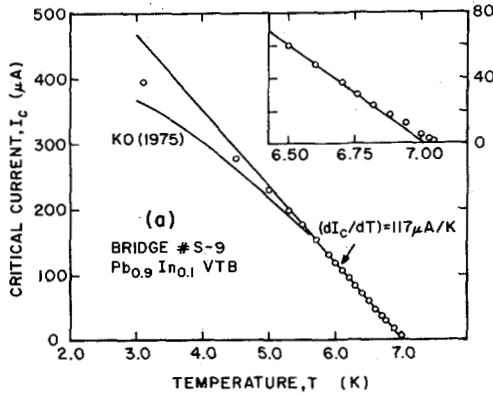


Fig. 2 $I_c(T)$ for $\text{Pb}_{0.9}\text{In}_{0.1}$ bridge S-9. Kulik-Omelyanchuk theory result scaled to slope at $0.9 T_c$.

Fig. 2. The data near T_c is linear in $(T_c - T)$, and at lower temperatures is closer to the predictions of Kulik and Omelyanchuk⁷ for small, dirty microbridges at arbitrary temperatures. The deviation from linearity very near T_c of $I_c(T)$ for the Pb-In bridges, seen in the inset of Fig. 1, is somewhat larger than the film transition width of ~ 25 mK. For alloy films, such a width is indicative of good film quality. The $I_c(T)$ data for the narrower In bridges lie very close to the theoretical results,⁷ and no deviation from linearity is seen near T_c .

While the linear temperature dependence of I_c observed for $0.75 < t < 0.95$ is in good agreement with the small bridge calculations,⁶ all the theories predict

$$R(dI_c/dT) = 0.64 \text{ mV/K.} \quad (1)$$

For R , we have chosen R_d , the minimum differential resistance on the finite-voltage part of the $V(I)$ curve, at $t = 0.99$. At this temperature, the Joule heating is minimal and the minimum differential resistance is nearly independent of temperature. The results for the product $R_d(dI_c/dT)$ are shown in Fig. 3. $R_d(dI_c/dT)$ decreases smoothly with decreasing bridge cross-section, and is close to the theoretical limit (Eq. (1)) for the bridges with the smallest normalized cross-sections $Wd/\xi(0)^2$. In contrast, we find that the product $R_{\text{tot}}(dI_c/dT)$, where R_{tot} is the total resistance of the bridge plus banks just above T_c , shows wide fluctuations which are correlated with variations in the bank thickness. We thus find that R_d is the most appropriate parameter for the bridge resistance.

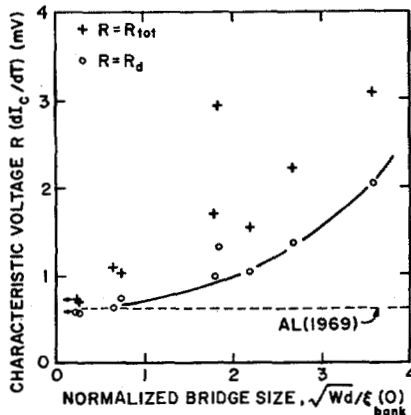


Fig. 3 $R(dI_c/dT)$ vs. (normalized bridge area)^{1/2} for all bridges. Pb-In bridges all have normalized areas > 1 . Solid line is a visual guide only. Theory result from Aslamazov and Larkin, Eq. 1. Bridge thickness = d .

Table I. Film Material Parameters

Material	T_c (K)	ρ (Ω cm)	$\xi(0)^a$
$\text{Pb}_{0.9}\text{In}_{0.1}$	7.1	7×10^{-6}	250 Å
In	3.42	7×10^{-7}	1660 Å

a. $\xi(0)$ is for the bank film; within the In bridges, the coherence length $\xi_b(0)$ is smaller.

For all the Pb-In bridges studied, the bridge resistance, R_d , is ≥ 2 times larger than $\rho L/Wd$, the calculated normal-state resistance of the bridge, R_n . (The bridge resistivity is equal to that of the bank film, as the resistivity ratios and T_c values are the same.) It is likely that $R_d > R_n$ because the quasiparticle potential gradient extends into the banks,⁹ and also because the superconducting wavefunction in the banks is partially depaired near the bridge ends.^{6,9} Bridges which are much thinner would avoid these complications.

IV. I-V CURVES AND JOULE HEATING

$V(I)$ curves of typical microbridges of Pb-In and of In are shown in Fig. 4(a) and (b). Near T_c the curves are roughly like those of the resistively-shunted-junction (RSJ) model, though the finite-voltage section does not extrapolate to $I = 0$. In addition, significant structure is seen in the dV/dI curves (not shown). The structure is due in part to cavity-related resonances, and for the In bridges, to energy-gap-related interactions at voltages $V_m = 2\Delta/m_e$, discussed later.

At somewhat lower temperatures, a region of constant differential resistance, or "foot", develops for $I \gtrsim I_c$. From the systematics of this feature we believe it is due to quasiparticle relaxation effects,⁴ as discussed by Octavio et al.¹⁰ and Schmid et al.¹⁰ For the In bridges, both the temperature dependence of the "foot" resistance, R_f , and the voltage at which it terminates agree with the theoretical predictions.¹⁰

In the $V(I)$ curves of our very narrow Pb-In bridges (S-6, 9, and 10), we find the low-voltage feature shown in Fig. 4(a), which may be interpreted as a foot. The increase in differential resistance at the end of the foot occurs at a voltage $V_f \approx 100 \mu\text{V}$, in reasonable agreement with the expected value of $80 \mu\text{V}$.¹⁰ However, R_f is equal to the device resistance R_d at all temperatures where the foot is observed, in contrast to the theoretical expectation. Studies on larger, pure Pb microbridges by other workers^{10,11} have not reported any low-voltage foot feature.

At the lowest temperatures, hysteresis in the $V(I)$ curves is observed for all the Pb-In bridges and In bridges, except the highest resistance In bridge, S-14, shown in Fig. 4(b). This bridge is non-hysteretic to the lowest temperature studied, 1.4 K. This is at least partly due to the three-dimensional cooling of the thick banks. The I-V curves of this bridge are among the most uniform, over a wide temperature range, of any microbridge discussed in the literature.

It is well established^{1,12} that hysteresis of the I-V curve of a microbridge can result from Joule heating. For $I > I_c$, a hot spot develops which persists until the current is reduced to $I_h < I_c$. Such hysteresis is undesirable, as it can preclude use in most analog applications, and can lead to excess noise.¹³

Figure 4(a) illustrates the development of hysteresis in a narrow Pb-In microbridge at low tempera-

tures. Due to the foot structure, the hysteresis first appears at a small finite voltage rather than at I_c . The hysteresis-free temperature range $\Delta T_{\text{no hyst}}$ is listed in Table II for all bridges studied. The series of Pb-In bridges clearly shows that $\Delta T_{\text{no hyst}}$ increases as the minimum cross-sectional area Wd decreases (e.g., compare S-6 to S-7). On the other hand, there is no strong correlation between thick banks and large $\Delta T_{\text{no hyst}}$. (The single exception to this rule is bridge S-8 for which $D \approx W$.) It must be that three-dimensional heat flow in the region near the bridge is the dominant source of thermal resistance when the bridge is biased just above its critical current.

The shunted bridge S-10 demonstrates that a small $I_c R$ product can be of value in reducing Joule heating (i.e., increasing $\Delta T_{\text{no hyst}}$), at a given bias current. This bridge had values of I_c and R_d appropriate for a 21Ω bridge in parallel with a 14Ω nonsuperconducting shunt, and $\Delta T_{\text{no hyst}} = 3.9$ K. It is likely that during storage at room temperature for a few weeks, a stress-induced hillock or whisker of In formed the shunt, which was nonsuperconducting at 6-7 K. During later testing, excessive microwave power apparently burned out the bridge, leaving the 14Ω normal resistance intact. While the reduced $I_c R$ product is helpful in reducing heating, it will also lead to a degraded signal-to-noise ratio and curtailed frequency response.

The In bridges show the same general trend as the Pb-In bridges. The dependence of $\Delta T_{\text{no hyst}}$ on cross-sectional area is even stronger for these bridges, because the scattering increases the bridge resistance, thus decreasing the power dissipation $\propto V^2/R_d$, without proportionately increasing the thermal resistance of the banks. (Recall that $V_c \equiv I_c R$ is roughly independent of the bridge resistance.)

A more direct and quantitative probe of the effects of Joule heating is provided by the energy-gap-related structure in the dV/dI curves, at voltages $V_m = 2\Delta/m\epsilon$. This structure is seen only for the In bridges, but not the Pb-In or In-Pb alloy bridges. It thus appears that dirty banks, $\frac{1}{2} < \frac{0.5}{BCS}$, prohibit the gap-related structure.

The gap value inferred from the third-order (i.e., $m=3$) or higher-order peaks, all of which occur at relatively low voltages, is in good agreement with the energy gap at the bath temperature, computed from $2\Delta(0) = 3.63 kT_c$. The first- and second-order peaks, however, occur at lower voltages than those predicted on the basis of the bath-temperature gap. This being so, an effective temperature $T_{\text{eff}} = T_b + \Delta T_{\text{sgs}}$ may be inferred from each peak of the gap structure. T_b is the substrate temperature. Octavio et al.¹² have shown that the gap structure reflects the local temperature a distance $\xi(T_b)$ from the bridge, so that

Table II. Microbridge Parameters and Performance Data

	L(Å)	W(Å)	D(Å)	$R_d(\Omega)$	ΔT (K)	V (mV)	P_o (μW)
					no hyst	max	
Pb-In							
S-6	600	500	2400	6.4	1.0	1.4	0.16
S-7	500	750	2400	3.9	0.5	>1.0	0.22
S-8	700	~700	750	6.9	0.6	>0.7	0.07
S-9	400	500	1100	8.4	1.2	1.5	0.12
S-10 ^a	400	400	1100	8.4	~3.9	>1.0	0.12
S-11	<300	800	6000	3.6	0.2	0.8	0.15
In							
S-13	2000	400	3500	2.0	1.0	>0.6	0.17
S-14	2000	<400	3500	5.1	>2.0	1.9	0.21
S-15	900	1800	3500	0.15	0.3	>0.3	0.6

Notes: Width at narrowest point, W , is listed. In general, the bridge thickness, d , is $\leq W$. Exceptions are S-9 ($d \sim 300\text{\AA}$) and S-15 ($d = 800\text{\AA}$). Bank thickness = D . a. Shunted bridge; see text.

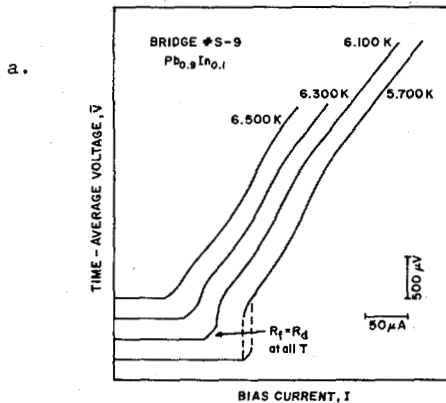
$$\Delta T_{\text{sgs}} = \frac{IV}{2\kappa\Omega\xi(T_b)}, \quad (2)$$

with κ the thermal conductivity and Ω the cooling solid angle for each bank. Our plots of ΔT_{sgs} vs. $IV/\xi(T_b)$ are roughly linear.⁴ However, the slope of the plot implies $\Omega\kappa \approx 1.2 \times 10^{-2} \text{ W/cm-K}$, which is an order of magnitude smaller than the result expected from the Wiedemann-Franz law, assuming κ is that of the bank film and that simple radial cooling occurs. The same numerical discrepancy is found for the maximum voltage of microwave-induced steps, discussed later.

V. EFFECTS OF MICROWAVE IRRADIATION

The $V(I)$ curves of all of our microbridges show many constant-voltage steps under microwave irradiation. The plots of step width ΔI_n vs. microwave amplitude are qualitatively similar to those obtained from the RSJ model. However, the steps gradually vanish as the microwave power becomes large.

The improvement of microwave response over that of Pb-In uniform-thickness bridges⁵ is due to the thick banks, which reduce the effects of Joule heating. The parameter V_{max} , the voltage of the highest observable microwave step, is a measure of the microwave response. V_{max} at low temperatures is listed for each bridge in Table II. Some of the best bridges were not tested at high enough microwave power or low enough temperature to establish V_{max} exactly, so a lower bound is tabulated. As with $\Delta T_{\text{no hyst}}$, V_{max} increases as the cross-



b.

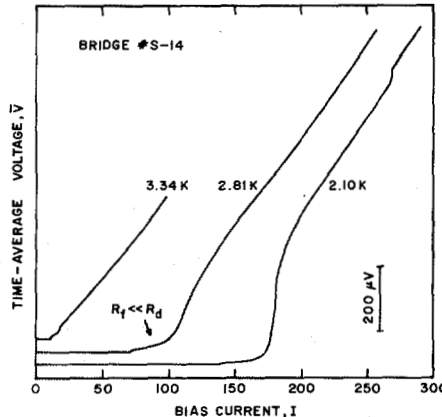


Fig. 4 $V(I)$ curves for:
a. Pb-In bridge S-9, and
b. In bridge S-14. For 2.1 K curve, the structure at 0.9 mV is a gap-related feature; see text.

sectional area, Wd , decreases. However, V_{\max} is also sensitive to the bank thickness D . For example, compare bridges S-8 and S-9.

As the bath temperature is reduced, V_{\max} increases to a saturation level which depends in part on bridge cross-section. V_{\max} for the wide bridge S-11 reaches saturation at $t = 0.90$, while V_{\max} for the narrow bridge S-6 is still increasing at that temperature. Near T_c , V_{\max} is nearly equal for the two bridges.

Experimental values of P_0 for $T = 0$, with P_0 the characteristic heating power introduced by Tinkham et al.², are listed in Table II. To determine $P_0(T = 0)$, the measured value of $V_{\max}(t = 0.90)$ and the Ginzburg-Landau temperature dependences were used. We estimated that V_{\max} corresponds to $I_c(P)/I_c(0) = 0.03$. The theoretical value of P_0 for the $Pb_{0.9}In_{0.1}$ bridges is $P_0 = 1.0 \times 10^{-6}W$, and for our In bridges, $P_0 = 4.7 \times 10^{-6}W$ is computed. Clearly, the experimentally obtained values of P_0 are about an order of magnitude smaller than the theoretical predictions. This may occur because the banks are not sufficiently thick for three-dimensional cooling in the large-heating regime, or for the In bridges, because the banks are dirtier near the bridge than far from the bridge. Another possible source of discrepancy is that the theory² assumes that the temperature distribution is the same as if the whole constriction (bridge plus banks) were nonsuperconducting. In fact, no power is dissipated in the regions of the banks which are superconducting, which nonetheless contribute thermal resistance. In the two In bridges S-13 and 14, the limitation on V_{\max} due to the bridge term² may also be significant. Thus, while the clean-dirty-clean effect produced by scattering in the bridge does provide reduced Joule heating, the improvement in performance is not as great as one might expect.

Three types of microwave-induced behavior which are not predicted by the RSJ model or simple Joule heating theories were also observed in this work. These include microwave-induced enhancement of the critical current, subharmonic steps (i.e., constant-voltage steps at $V = nhf/2me$ with m an integer), and microwave-induced asymmetry of the $V(I)$ curves, observed for all bridges tested. This asymmetry of the positive and negative I-V curves displays a number of reproducible and systematic trends. The details of the asymmetry are reproducible after warming to room temperature, but are sensitive to changes in the microwave source apparatus. We believe that the asymmetry is an intrinsic effect which deserves further study. The various non-RSJ effects are discussed in detail in Ref. 4.

To assess the relative performance of our microbridges, we may compare them to the best-case results reported in the literature, for small VTBs of Sn^{12} , Pb^{11} , Nb^{14} , and NbN^{15} . Large values of V_{\max} and $\Delta T_{no\ hyst}$ are achieved for these bridges and those in Table II, e.g. S-9 and 14. However, to simultaneously achieve a high resistance, ≥ 5 to 10 ohms, it is necessary that the bridge be very small and of a high-resistivity material (our Pb-In bridges, Refs. 14, 15), or that significant boundary scattering occur in the bridge (our In bridges).

Most of the bridges^{11,12}, like ours, operate in the well-studied depairing regime⁶, with $L \lesssim \xi(T)$; however, only the ultrasmall bridges discussed in this work achieve $R \sim 100$. The mechanisms of the Josephson effect for the other high-resistance bridges, of Nb and NbN, involve granular-superconductor effects. These granular mechanisms are not well studied theoretically, though the devices appear to work well in practice. Indeed, the shortest Nb bridge, 1200Å long, appears to

work well at $\sim \frac{1}{2}T_c$ because its I_cR product, 0.3 mV, is much smaller than the theoretical prediction (Ref. 6). An understanding of the behavior of those devices will require further study.

VI. CONCLUSIONS

In this work we have studied the properties of ultrasmall variable-thickness microbridges. These bridges display most of the characteristics desired for Josephson device applications: high electrical resistance and reasonably wide temperature and voltage operating ranges. As the cross-sectional area is reduced, the properties show many of the improvements expected, and effects of scattering within the bridge become evident in the smaller In bridges. We have demonstrated that high-resistance Pb-based devices, with $T_c > 4.2$ K, can be reliably fabricated, and that high-resistance alloys can be utilized, if the requisite sub-1000Å lithography is accomplished.

This work signifies considerable progress toward the goal of microbridges with the characteristics of high-quality point contacts, and confirms a number of theoretical expectations. However, the microbridges we have produced are not yet fully perfected. Values of P_0 are uniformly below the theoretical prediction. What appears to be required is a significantly thinner bridge, still of high resistance, with clean, thick banks. These objectives do appear to be attainable with advanced lithographic techniques currently available. The results of this work provide strong encouragement for such efforts.

This research was supported in part by NSF grants ENG 77-10164 and ECS 79-27165. We thank A. S. Pooley and P. Male for skilled assistance with scanning electron microscopy. The use of clean room facilities at Yale is also acknowledged.

REFERENCES

1. M. Tinkham, AIP Conf. Proc. **44**, 269 (1978); W. J. Skocpol, AIP Conf. Proc. **44**, 335 (1978).
2. M. Tinkham, M. Octavio, and W. J. Skocpol, J. Appl. Phys. **48**, 1311 (1977).
3. M. D. Feuer and D. E. Prober, Appl. Phys. Lett. **36**, 226 (1980).
4. M. D. Feuer, Ph.D. Thesis, Yale Univ., 1980, and M. D. Feuer and D. E. Prober, to be published.
5. M. D. Feuer and D. E. Prober, IEEE Trans. MAG-**15**, 578 (1979).
6. K. K. Likharev, Rev. Mod. Phys. **51**, 101 (1979).
7. I. O. Kulik and A. N. Omelyanchuk, JETP Lett. **21**, 96 (1975). For the pure In bridges S-13 and 14, the dirty-material formulas apply because $\lambda < \xi_{BCS}$.
8. R. D. Chaudhari and J. B. Brown, Phys. Rev. **139**, A1482 (1965).
9. G. Daalmans, T. M. Klapwijk, and J. E. Mooij, IEEE Trans. MAG-**13**, 719 (1977).
10. M. Octavio, W. J. Skocpol, and M. Tinkham, Phys. Rev. B17, 159 (1978); Albert Schmid, Gerd Schön, and Michael Tinkham, Phys. Rev. **B21**, 5076 (1980).
11. J. T. C. Yeh and R. A. Buhrman, J. Appl. Phys. **48**, 5360 (1978).
12. M. Octavio, W. J. Skocpol, and M. Tinkham, IEEE Trans. MAG-**13**, 739 (1977); M. Octavio and W. J. Skocpol, J. Appl. Phys. **50**, 3505 (1979).
13. T. W. Lee, Ph.D. Thesis, SUNY-Stonybrook (1977).
14. R. B. Laibowitz, A. N. Broers, J.T.C. Yeh and J.M. Viggiano, Appl. Phys. Lett. **35**, 891 (1979); R. B. Laibowitz et al., AIP Conf. Proc. **58**, 278 (1980).
15. J. H. Claassen, Appl. Phys. Lett. **36**, 771 (1980).